Molecular Cell
Article

Histone Methylation by PRC2 Is Inhibited by Active Chromatin Marks

Frank W. Schmitges,[1,6] Archana B. Prusty,[2,6] Mahamadou Faty,[1] Alexandra Stützer,[3] Gondichatnahalli M. Lingaraju,[1] Jonathan Aiwazian,[1] Ragna Sack,[1] Daniel Hess,[1] Ling Li,[4] Shaolian Zhou,[4] Richard D. Bunker,[1] Urs Wirth,[5] Tewis Bouwmeester,[5] Andreas Bauer,[5] Nga Ly-Hartig,[2] Kehao Zhao,[4] Homan Chan,[4] Justin Gu,[4] Heinz Gut,[1] Wolfgang Fischle,[3] Jürg Müller,[2,7,*] and Nicolas H. Thomä[1,*]

[1]Friedrich Miescher Institute for Biomedical Research, Maulbeerstrasse 66, CH-4058 Basel, Switzerland
[2]Genome Biology Unit, EMBL Heidelberg, Meyerhofstrasse 1, D-69117 Heidelberg, Germany
[3]Laboratory of Chromatin Biochemistry, Max Planck Institute for Biophysical Chemistry, Am Fassberg 11, D-37077 Göttingen, Germany
[4]China Novartis Institutes for Biomedical Research, Lane 898 Halei Road, Zhangjiang, Shanghai, China
[5]Novartis Institutes for Biomedical Research, CH-4002 Basel, Switzerland
[6]These authors contributed equally to this work
[7]Present address: Max Planck Institute of Biochemistry, Am Klopferspitz 18, D-82152 Martinsried, Germany
*Correspondence: muellerj@biochem.mpg.de (J.M.), nicolas.thoma@fmi.ch (N.H.T.)
DOI 10.1016/j.molcel.2011.03.025

SUMMARY

The Polycomb repressive complex 2 (PRC2) confers transcriptional repression through histone H3 lysine 27 trimethylation (H3K27me3). Here, we examined how PRC2 is modulated by histone modifications associated with transcriptionally active chromatin. We provide the molecular basis of histone H3 N terminus recognition by the PRC2 Nurf55-Su(z)12 submodule. Binding of H3 is lost if lysine 4 in H3 is trimethylated. We find that H3K4me3 inhibits PRC2 activity in an allosteric fashion assisted by the Su(z)12 C terminus. In addition to H3K4me3, PRC2 is inhibited by H3K36me2/3 (i.e., both H3K36me2 and H3K36me3). Direct PRC2 inhibition by H3K4me3 and H3K36me2/3 active marks is conserved in humans, mouse, and fly, rendering transcriptionally active chromatin refractory to PRC2 H3K27 trimethylation. While inhibition is present in plant PRC2, it can be modulated through exchange of the Su(z)12 subunit. Inhibition by active chromatin marks, coupled to stimulation by transcriptionally repressive H3K27me3, enables PRC2 to autonomously template repressive H3K27me3 without overwriting active chromatin domains.

INTRODUCTION

Polycomb (PcG) and trithorax group (trxG) proteins form distinct multiprotein complexes that modify chromatin. These complexes are conserved in animals and plants and are required to maintain spatially restricted transcription of HOX and other cell fate determination genes (Henderson and Dean, 2004; Pietersen and van Lohuizen, 2008; Schuettengruber et al., 2007; Schwartz and Pirrotta, 2007). PcG proteins act to repress their target genes while trxG protein complexes are required to keep the same genes active in cells where they must be expressed.

Among the PcG protein complexes, Polycomb repressive complex 2 (PRC2) is a histone methyl-transferase (HMTase) that methylates Lys27 of H3 (H3K27) (Cao et al., 2002; Czermin et al., 2002; Kuzmichev et al., 2004; Müller et al., 2002). High levels of H3K27 trimethylation (H3K27me3) in the coding region generally correlate with transcription repression (Cao et al., 2008; Nekrasov et al., 2007; Sarma et al., 2008). PRC2 contains four core subunits: Enhancer of zeste [E(z), EZH2 in mammals], Suppressor of zeste 12 [Su(z)12, SUZ12 in mammals], Extra-sex combs [ESC, EED in mammals] and Nurf55 [Rbbp4/RbAp48 and Rbbp7/RbAp46 in mammals] (reviewed in Schuettengruber et al., 2007; Wu et al., 2009). E(z) is the catalytic subunit; it requires Nurf55 and Su(z)12 for nucleosome association, whereas ESC is required to boost the catalytic activity of E(z) (Nekrasov et al., 2005). Recent studies reported that ESC binds to H3K27me3 and that this interaction stimulates the HMTase activity of the complex (Hansen et al., 2008; Margueron et al., 2009; Xu et al., 2010). The observation that PRC2 is able to bind to the same modification that it deposits led to a model for propagation of H3K27me3 during replication. In this model, recognition of H3K27me3 on previously modified nucleosomes promotes methylation of neighboring nucleosomes that contain newly incorporated unmodified histone H3 (Hansen et al., 2008; Margueron et al., 2009). However, it is unclear how such a positive feedback loop ensures that H3K27 trimethylation remains localized to repressed target genes and does not invade the chromatin of nearby active genes.

In organisms ranging from yeast to humans, chromatin of actively transcribed genes is marked by H3K4me3, H3K36me2, and H3K36me3 modifications: while H3K4me3 is tightly localized at and immediately downstream of the transcription start site, H3K36me2 peaks adjacently in the 5′ coding region and H3K36me3 is specifically enriched in the 3′ coding region (Bell et al., 2008; Santos-Rosa et al., 2002). Among the trxG proteins that keep PcG target genes active are the HMTases Trx and Ash1, which methylate H3K4 and H3K36, respectively (Milne et al., 2002; Nakamura et al., 2002; Tanaka

et al., 2007). Studies in *Drosophila* showed that Trx and Ash1 play a critical role in antagonizing H3K27 trimethylation by PRC2, suggesting a crosstalk between repressive and activating marks (Papp and Müller, 2006; Srinivasan et al., 2008).

In this study we investigated how PRC2 activity is modulated by chromatin marks typically associated with active transcription. We found that the Nurf55 WD40 propeller binds the N terminus of unmodified histone H3 and that H3K4me3 prevents this binding. In the context of the tetrameric PRC2 complex, we find that H3K4me3 and H3K36me2/3 (i.e., both H3-K36me2 and H3-K36me3) inhibit histone methylation by PRC2 in vitro. Dissection of this process by using fly, human, and plant PRC2 complexes suggests that the Su(z)12 subunit is important for mediating this inhibition. PRC2 thus not only contains the enzymatic activity for H3K27 methylation and a recognition site for binding to this modification, but it also harbors a control module that triggers inhibition of this activity to prevent deposition of H3K27 trimethylation on transcriptionally active genes. PRC2 can thus integrate information provided by pre-existing histone modifications to accurately tune its enzymatic activity within a particular chromatin context.

RESULTS

Structure of Nurf55 Bound to the N Terminus of Histone H3

Previous studies reported that Nurf55 alone is able to bind to histone H3 (Beisel et al., 2002; Hansen et al., 2008; Song et al., 2008; Wysocka et al., 2006) but not to a GST-H3 fusion protein (Verreault et al., 1998). By using fluorescence polarization (FP) measurements, we found that Nurf55 binds the very N terminus of unmodified histone H3 encompassing residues 1–15 ($H3_{1-15}$) with a K_D of ~0.8 ± 0.1 μM but does not bind to a histone $H3_{19-38}$ peptide (Figure 1A). Crystallographic screening resulted in the successful cocrystallization of Nurf55 in complex with an $H3_{1-19}$ peptide. After molecular replacement with the known structure of Nurf55 (Song et al., 2008), the initial $mF_o - DF_c$ difference map showed density for H3 residues 1–14 in both Nurf55 molecules in the crystallographic asymmetric unit. Figures 1B–1E show the structure of $H3_{1-19}$ bound to *Drosophila* Nurf55, refined to 2.7 Å resolution (R/R_{free} = 20.1% and 25.0%, Table 1; Figure S1A, available online). The H3 peptide binds to the flat surface of the Nurf55 WD40 propeller (Figure 1B), subsequently referred to as the canonical binding site (*c*-site) (Gaudet et al., 1996). The H3 peptide is held in an acidic pocket (Figures 1C and 1E) and traverses the central WD40 cavity in a straight line across the propeller (Figure 1B).

Nurf55 binds the H3 peptide by contacting H3 residues Ala1, Arg2, Lys4, Ala7, and Lys9. Each of these residues forms side-chain specific contacts with the Nurf55 propeller (Figures 1D and 1E). The bulk of the molecular recognition is directed toward H3 Arg2 and Lys4. Ala1 sits in a buried pocket with its α-amino group hydrogen bonding to Nurf55 Asp252, which recognizes and fixes the very N terminus of histone H3. The neighboring Arg2 is buried deeper within the WD40 propeller fold, with its guanidinium group sandwiched by Nurf55 residues Phe325 and Tyr185 (Figure 1D). H3 Lys4 binds to a well-defined surface pocket on Nurf55 located on blade 2, near the central cavity of the propeller. Its ε-amino group is specifically coordinated by the carboxyl groups of Nurf55 residues Glu183 and Glu130 and through the amide oxygen of Asn132 (Figure 1E). Lys9 is stabilized by hydrophobic interactions on the WD40 surface while having its ε-amino group held in solvent-exposed fashion (Figure 1D). Ser10 of histone H3 marks the beginning of a turn that inverses the peptide directionality. Histone H3 residues Thr11–Lys14 become progressively disordered and are no longer specifically recognized. No interpretable density was observed beyond Lys14. Taken together, Nurf55 specifically recognizes an extended region of the extreme N terminus of histone H3 (11 residues long, 700 $Å^2$ buried surface area) in the canonical ligand binding location of WD40 propeller domains.

Structure of the Nurf55-Su(z)12 Subcomplex of PRC2

The H3-Nurf55 structure prompted us to investigate how Nurf55 might bind histone tails in the presence of Su(z)12, its interaction partner in PRC2 (Nekrasov et al., 2005; Pasini et al., 2004). As a first step we mapped the Nurf55-Su(z)12 interaction in detail by carrying out limited proteolysis experiments on reconstituted *Drosophila* PRC2, followed by isolation of a Nurf55-Su(z)12 subcomplex. Mass spectrometric analysis and pull-down experiments with recombinant protein identified Su(z)12 residues 73–143 [hereafter referred to as $Su(z)12_{73-143}$] as sufficient for Nurf55 binding (Figures S1C and S1D).

Crystals were obtained when *Drosophila* Nurf55 and Su(z)12 residues 64–359 were set up in the presence of 0.01% subtilisin protease (Dong et al., 2007). After data collection, the structure was refined to a maximal resolution of 2.3 Å (Table 1). Molecular replacement with Nurf55 as search model provided clear initial $mF_o - DF_c$ difference density for a 13 amino acid-long Su(z)12 fragment spanning Su(z)12 residues 79–91 (Figures 2A–2C). The final model was refined to 2.3 Å (R/R_{free} = 17.5%/20.9%) and verified by simulated annealing composite-omit maps (Figure S1B). The portion of Su(z)12 involved in Nurf55 binding will henceforth be referred to as the Nurf55 binding epitope (NBE). The Su(z)12 binding site on Nurf55 is located on the side of the propeller between the stem of the N-terminal α helix (α1) and the PP loop (Figures 2A and2B). Binding between Su(z)12 and Nurf55 occurs mostly through hydrophobic interactions in an extended conformation. The interaction surface between Nurf55 and the NBE is large for a peptide, spanning around 800 $Å^2$. Sequence alignment between Su(z)12 orthologs reveals that the NBE is highly conserved (53% identity and 84% similarity) in animals and in plants (Figure 2E). With the exception of Su(z)12 Arg85, the majority of the conserved Su(z)12 NBE residues engage in hydrophobic packing with Nurf55 (Figures 2B and 2C). Together with the Su(z)12 VEFS domain and the C_2H_2 zinc finger (C5 domain) (Birve et al., 2001), the NBE constitutes the only identifiable motif in Su(z)12 found conserved in all Su(z)12 orthologs.

The NBE binding site on Nurf55 has previously been shown to be occupied by helix 1 of histone H4 (Figure 2D) (Murzina et al., 2008; Song et al., 2008), an epitope not accessible in assembled nucleosomes (Luger et al., 1997). Nurf55 binds H4 and the Su(z)12 NBE epitope in a different mode, and importantly, with opposite directionality (Figure 2D). The detailed comparison of the Nurf55-Su(z)12 structure with that of H4 bound to Nurf55

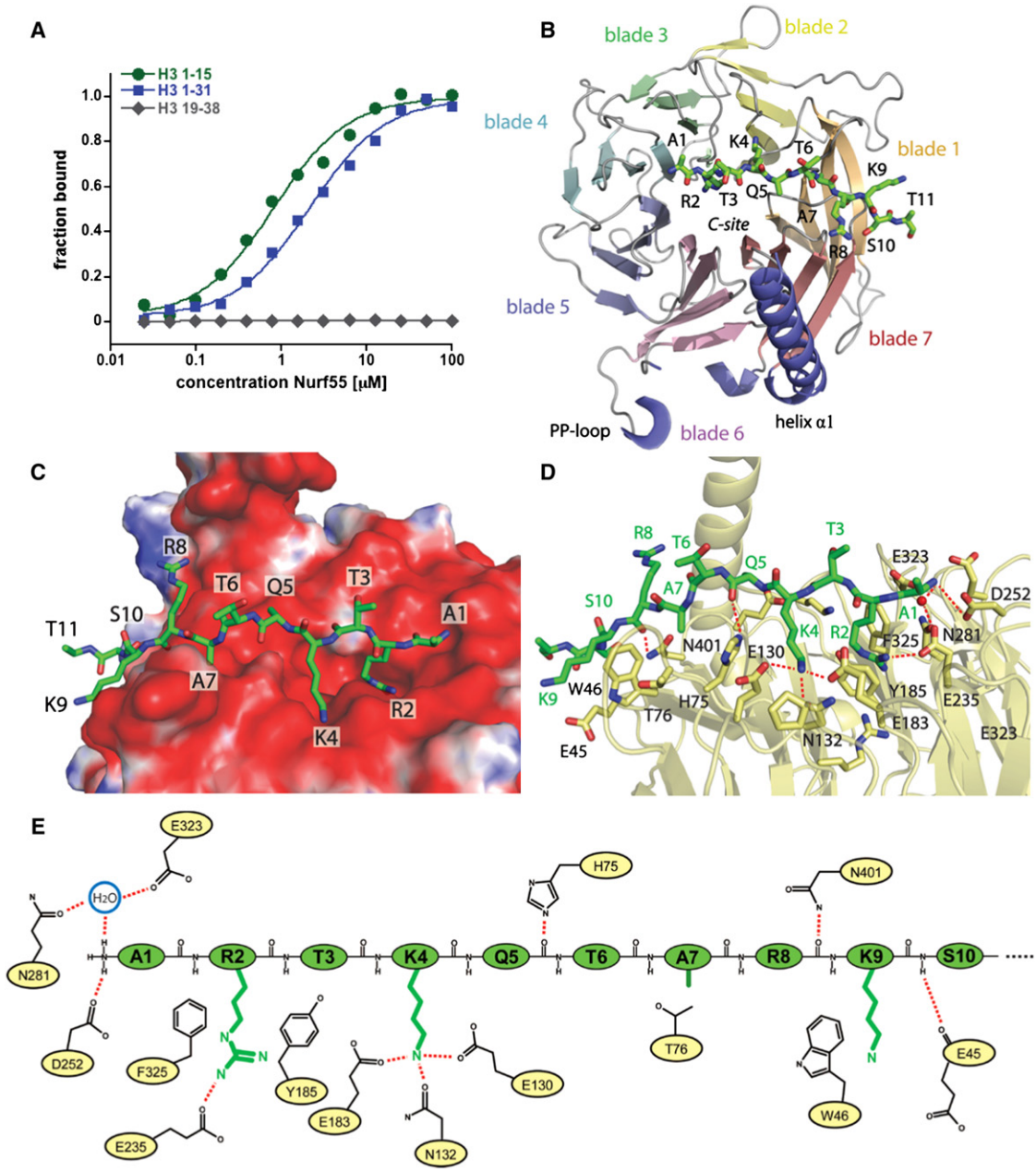

Figure 1. Crystal Structure of Nurf55 in Complex with a Histone $H3_{1–19}$ Peptide

(A) Nurf55 binds to an $H3_{1–15}$ peptide with an affinity of ~0.8 ± 0.1 μM as measured by FP. It has similar affinity for an $H3_{1–31}$ peptide (2.2 ± 0.2 μM) but no binding can be detected to an $H3_{19–38}$ peptide.

(B) Ribbon representation of Nurf55-$H3_{1–19}$. Nurf55 is shown in rainbow colors and $H3_{1–19}$ is depicted in green. The peptide is bound to the *c*-site of the WD40 propeller.

(C) Electrostatic surface potential representation (−10 to 10 kT/e) of the *c*-site with the H3 peptide shown as a stick model in green.

(D) Close-up of the *c*-site detailing the interactions between Nurf55 (yellow) and the $H3_{1–19}$ peptide (green), with a water molecule shown as a red sphere.

(E) Schematic representation of interactions between the $H3_{1–19}$ peptide (green) and Nurf55 (yellow).

strongly suggests that binding of Su(z)12 (NBE) and of H4 (helix 1) are mutually exclusive (Figure 2D). We therefore refer to the Su(z)12 and H4 binding site on Nurf55 as the *S/H*-site.

Su(z)12 fragments that include the NBE have poor solubility by themselves and generally require Nurf55 coexpression for solubilization. However, we were able to measure binding of a chemically synthesized $Su(z)12_{75–93}$ peptide to Nurf55 by isothermal titration calorimetry (ITC) and found that the peptide was bound with a K_D value of 6.7 ± 0.3 μM in a 1:1 stoichiometry (Figure 2F). Pull-down experiments with recombinant protein and

Table 1. Crystallographic Data and Refinement Statistics

	Nurf55 – Su(z)12	Nurf55 – $H3_{1–19}$
Space Group	$P2_12_12_1$	$P2_12_12_1$
Unit Cell Dimensions		
a, *b*, *c* (Å)	53.03, 87.19, 99.54	55.97, 88.15, 204.02
α, β, γ (°)	90.0, 90.0, 90.0	90.0, 90.0, 90.0
Resolution range (Å)	25.0 – 2.3 (2.38-2.30)[a]	37.7 – 2.7 (2.8-2.7)[a]
Percent complete	99.2 (92.0)[a]	96.6 (90.6)[a]
Redundancy	15.6 (12.4)[a]	6.4 (5.3)[a]
R_{sym}	0.074 (0.338)[a]	0.091 (0.428)[a]
$I/\sigma I$	43.3 (6.2)[a]	15.6 (4.6)[a]
Resolution (Å)	2.3	2.7
Number of reflections	20984	28271
R_{work}/R_{free}	0.175/0.209	0.201/0.250
Number of atoms	3315	6197
B-Factors	29.8	46.9
Protein	29	47.0
Water	38.3	38.1
RMS Deviations		
Bond lengths (Å)	0.008	0.003
Bond angles (°)	1.124	0.752

[a] The values for the data in the highest resolution shell are shown in parentheses.

streptavidin beads suggest that Su(z)12 residues 94–143 harbor an additional Nurf55 binding site not visible in the structure (Figure S1E). $Su(z)12_{144–359}$, lacking the N-terminal 143 residues, no longer binds to Nurf55. The NBE (residues 79–93) and the region adjacent to the NBE (residues 94–143) are thus required for stable interaction with Nurf55. The extended NBE was found enriched after limited proteolysis and in subsequent gel filtration runs coupled with quantitative mass spectrometry (Figure S1C). As the NBE was the only fragment visible after structure determination, we conclude that it represents the major Su(z)12 interaction epitope for Nurf55 binding.

The Nurf55-Su(z)12 Complex Binds to Histone H3

In order to study the potential interdependence of the identified Nurf55 binding sites we compared binding of Nurf55 and Nurf55-Su(z)12 to the histone H3 N terminus. FP experiments showed similar affinities for binding of a histone $H3_{1–15}$ peptide to Nurf55 (K_D ~0.8 ± 0.1 μM; Figure 1A) and a Nurf55-$Su(z)12_{73–143}$ complex (K_D ~0.6 ± 0.1 μM; Figure 2G). Importantly, mutation of Nurf55 residues contacting H3 via its *c*-site drastically reduced binding to an $H3_{1–15}$ peptide (Figure S2A), demonstrating that the Nurf55-$Su(z)12_{73–143}$ complex indeed binds the $H3_{1–15}$ peptide through the *c*-site. We conclude that the presence of Su(z)12 is compatible with Nurf55 binding to H3 via its *c*-site and that the two binding interactions are not interdependent.

The observation that the Su(z)12 NBE occupies the same Nurf55 pocket that was previously shown to bind to helix 1 of histone H4 prompted us to test whether the $Su(z)12_{73–143}$-Nurf55 complex could still bind to histone H4. We performed pull-down experiments with a glutathione S-transferase (GST) fusion protein containing histone $H4_{1–48}$ (Murzina et al., 2008) and found that H4 stably interacted with isolated Nurf55 but not with $Su(z)12_{73–143}$-Nurf55 (Figure 2H). In PRC2, the presence of Su(z)12 in the Nurf55 *S/H*-site therefore precludes binding to helix 1 of histone H4.

H3 Binding by Nurf55-Su(z)12 Is Sensitive to the Methylation Status of Lysine 4

We next investigated how posttranslational modifications of the H3 tail affect binding to the Nurf55-$Su(z)12_{73–143}$ complex. Modifications on H3 Arg2, Lys9, and Lys14 did not change affinity of Nurf55-Su(z)12 for the modified $H3_{1–15}$ peptide (Figures S2B and S2D). In contrast, peptides that were mono-, di-, or trimethylated on Lys4 were bound with significantly reduced affinity exhibiting K_D values of 17 ± 3 μM (H3K4me1), 24 ± 3 μM (H3K4me2), and >70 μM (H3K4me3), respectively (Figure 2I). The FP binding data were independently confirmed by ITC measurements (Figures S2C–S2F). Together, these findings are in accord with the structural data, which show that H3K9 and H3K14 are being held with their ε-amino moiety solvent-exposed, while the H3K4 side chain is tightly coordinated (Figure 1E). The additional methyl groups on the H3K4 ε-amino group are expected to progressively decrease affinity because of increased steric clashes within the H3K4 binding pocket.

H3K27 Methylation by PRC2 Is Inhibited by Histone H3K4me3 Marks

We then examined the effect of H3K4me3 modifications, which are no longer retained by Nurf55-Su(z)12, on the catalytic activity of PRC2. In a first set of experiments, we determined PRC2 steady-state parameters on histone $H3_{1–45}$ peptide substrates that were either unmodified or methylated at Lys 4. We observed similar K_M values for H3 and H3K4me3 peptides of 0.84 ± 0.21 μM and 0.36 ± 0.07 μM, respectively (Figure 3A), and similar K_M values for SAM (5.42 ± 0.65 μM for H3 and 10.04 ± 1.56 μM for H3K4me3). The turnover rate constant k_{cat}, however, was 8-fold reduced in the presence of H3K4me3: 2.53 ± 0.21 min^{-1} for unmodified H3 and 0.32 ± 0.08 min^{-1} in the presence of H3K4me3 (Figure 3A). While substrate binding is largely unaffected, turnover is thus severely inhibited in the presence of H3K4me3. This behavior, which results in a k_{cat}/K_M specificity constant of 7.8 × 10^3 $M^{-1}s^{-1}$ (unmodified H3) compared to 0.53 × 10^3 $M^{-1}s^{-1}$ (H3K4me3), is consistent with heterotrophic allosteric inhibition of the PRC2 HMTase triggered by the presence of the H3K4me3.

To investigate the effect of the H3K4me3 modification on PRC2 activity in the context of nucleosomes, we reconstituted mononucleosomes with a trimethyllysine analog (MLA) at Lys4 in H3 (referred to as H3Kc4me3; Figure S3A) (Simon et al., 2007). We found that total H3K27 methylation (measured by incorporation of ^{14}C-labeled methyl groups) was substantially impaired on H3Kc4me3-containing nucleosomes compared to wild-type nucleosomes (Figures S3B and S3C). We used western blot analysis to monitor how levels of H3K27 mono-, di-, and trimethylation were affected by the H3Kc4me3 modification. While H3K27me1 formation was reduced by more than 50% on H3Kc4me3 nucleosomes compared to unmodified nucleosomes (Figures 3B and 3C), H3K27 dimethylation and

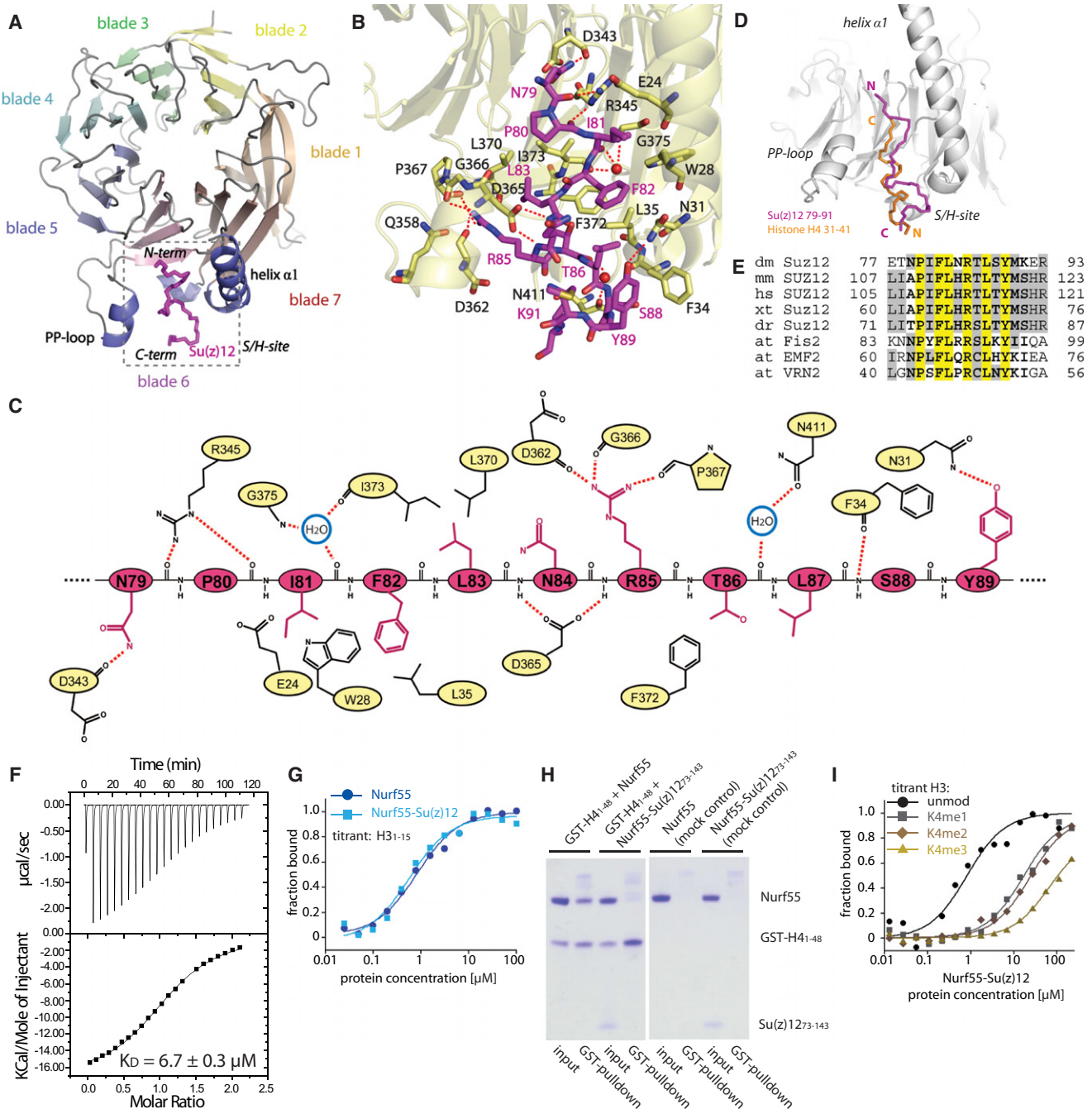

Figure 2. Crystal Structure and Characterization of Nurf55 in Complex with the Su(z)12 Binding Epitope for Nurf55

(A) Ribbon representation of Nurf55-Su(z)12. Nurf55 (rainbow colors) depicts the WD40 domain nomenclature and Su(z)12 is shown in magenta. The *S/H*-site is marked by a dashed box.

(B) Detailed interactions of Su(z)12 (magenta) with the *S/H*-site (yellow). Water molecules are depicted as red spheres.

(C) Schematic representation of interactions between Su(z)12 (magenta) and Nurf55 (yellow).

(D) Overlay of the backbone trace of Su(z)12 (magenta) and the H4 helix α1 (orange) (Song et al., 2008) in the *S/H*-site.

(E) Alignment of the Su(z)12 NBE with sequences from *Drosophila melanogaster* (dm, Q9NJG9), mouse (mm, NP_954666), human (hs, AAH15704), *Xenopus tropicalis* (xt, BC121323), zebrafish (dr, BC078293), and the three *Arabidopsis thaliana* (at) homologs Fis2 (ABB84250), EMF2 (NP_199936), and VRN2 (NP_567517). Identical residues are highlighted in yellow.

(F) ITC profile for binding of a $Su(z)12_{75–93}$ peptide to Nurf55. Data were fitted to a one-site model with stoichiometry of 1:1. The derived K_D value is 6.7 ± 0.3 μM.

(G) Binding of $H3_{1–15}$ to Nurf55 (0.8 ± 0.1 μM) and Nurf55-$Su(z)12_{73–143}$ (0.6 ± 0.1 μM) measured by FP.

A

Substrate	Apparent Km of SAM (μM)	Apparent Km of peptide (nM)	k_{cat} (min^{-1})	k_{cat}/Km ($M^{-1}S^{-1}$)
$H3_{1-45}$ -biotin	5.42 ± 0.65	836 ± 207	2.53 ± 0.21	7.8×10^3
$H3K4me3_{1-45}$ -biotin	10.04 ± 1.56	355 ± 74.6	0.32 ± 0.08	0.53×10^3

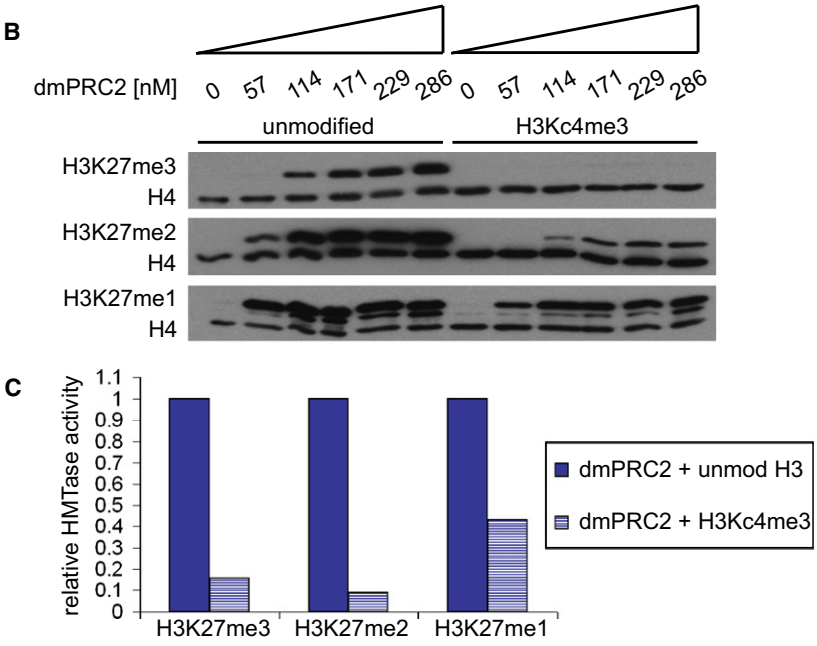

Figure 3. HMTase Activity of PRC2 Is Inhibited by H3K4me3 Marks

(A) HMTase assay with PRC2 and $H3_{1-45}$-biotin peptides measuring the concentration of SAH produced by the enzymatic reaction. When an H3K4me3-modified peptide is used, the specificity constant (k_{cat}/K_M) is drastically reduced, indicative of heterotrophic allosteric inhibition.

(B) Western blot-based HMTase assay by using recombinant *Drosophila* mononucleosomes (571 nM) and increasing amounts of PRC2. HMTase activity was monitored with antibodies against H3K27me1, H3K27me2, or H3K27me3 as indicated; in each case the membrane was also probed with an antibody against unmodified histone H4 to control for equal loading and western blot processing. Deposition of K27 di- and trimethylation is drastically reduced when nucleosomes are used that carry a H3Kc4me3 modification.

(C) Quantification of HMTase activity of *Drosophila* PRC2 (286 nM) on unmodified and H3Kc4me3-modified nucleosomes by quantitative western blotting.

trimethylation were impaired by more than 80% by using H3Kc4me3 nucleosomes (Figure 3C). In order to ascertain that inhibition of PRC2 is indeed due to trimethylation of the amino group in the lysine side chain, and not due to the use of the MLA, we performed HMTase assays on H3K4me3-containing nucleosomes generated by native peptide ligation (Shogren-Knaak et al., 2003) and on H3Kc4me0 and H3K4A nucleosomes. H3K27 mono-, di-, and trimethylation was comparably inhibited on H3K4me3 and on H3Kc4me3-containing nucleosomes, but was not affected by H3Kc4me0 and H3K4A (Figures S3D and S3E). We conclude that H3K4me3 specifically inhibits PRC2-mediated H3K27 methylation with the most pronounced inhibitory effects observed for H3K27 di- and trimethylation.

We next tested whether the H3K4me3 modification affects PRC2 nucleosome binding. In electrophoretic mobility shift assays (EMSA), we found that PRC2 binds unmodified or H3Kc4me3-modified nucleosomes with comparable affinity (Figure S4A). Even though binding of Nurf55 to the N terminus of histone H3 is almost 100-fold reduced by H3K4me3 (Figure 2I and Figure S2F), interaction of the Nurf55 *c*-site with H3K4 does not seem to make a detectable contribution to nucleosome binding by PRC2 in this assay. Consistent with the allosteric mechanism of H3K4me3 inhibition that we had observed in the peptide assays (Figure 3A), inhibition of the PRC2 HMTase activity by H3K4me3-containing nucleosomes is not caused by impaired nucleosome binding, but is rather the consequence of reduced catalytic turnover.

H3K4me3 Needs to Be Present on the Same Tail as K27 to Inhibit PRC2

We then assessed whether inhibition of the PRC2 HMTase activity by H3K4me3 requires the K4me3 mark to be located on the substrate nucleosome (in *cis*), or whether it could also be triggered if the H3K4me3 modification was provided on a separate peptide (in *trans*). We performed HMTase assays on unmodified oligonucleosomes in the presence of increasing amounts of a histone $H3_{1-15}$ peptide trimethylated at K4 ($H3_{1-15}$-K4me3) (Figure 4A). Addition of the $H3_{1-15}$-K4me3 peptide did not affect PRC2 HMTase activity at peptide concentrations as high as ~200 μM. When testing $H3_{1-19}$-unmodified peptide in controls at comparable concentrations, we did observe concentration-dependent PRC2 inhibition (Figure 4A), probably because of substrate competition at large peptide excess. As H3K4me3-

(H) GST pull-down assay with recombinant GST-$H4_{1-48}$ and Nurf55 and Nurf55-Su(z)12_{73-143} proteins. GST-$H4_{1-48}$ is able to bind Nurf55 alone but in the Nurf55-Su(z)12_{73-143} complex the binding site is occupied by Su(z)12 (left panel). Control pull-downs with GST beads and either Nurf55 or Nurf55-Su(z)12_{73-143} alone showed no unspecific binding (right panel).

(I) Binding of different $H3_{1-15}$ peptides to Nurf55-Su(z)12_{73-143} measured by FP. While unmodified H3 is bound with 0.8 ± 0.1 μM affinity, methylation of Lys 4 drastically reduces binding affinity (17 ± 3 μM for K4me1, 24 ± 3 μM for K4me2, and >70 μM for K4me3).

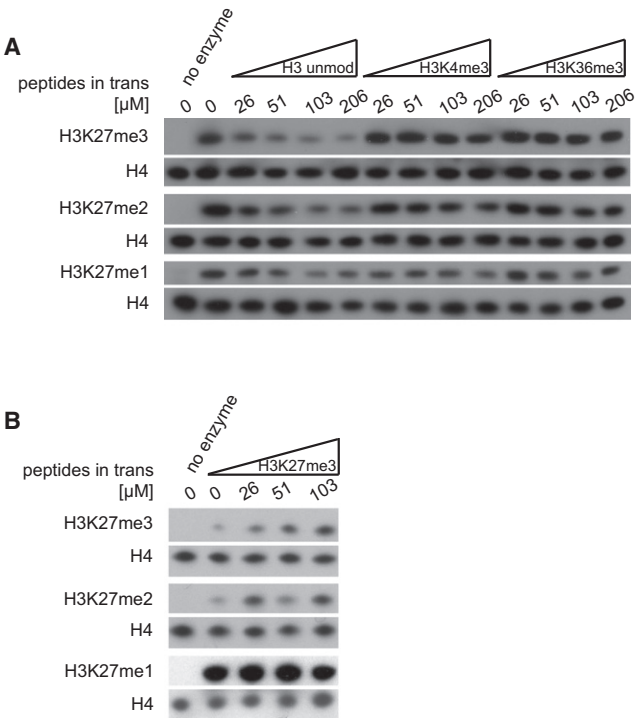

Figure 4. PRC2 Activity Is Not Inhibited by H3K4me3 Peptides in *trans*

(A) Western blot-based HMTase assay by using unmodified 4-mer oligonucleosomes (36 nM) and increasing amounts of H3 peptides added in *trans*. Enzyme concentration was kept constant at 86 nM. Western blots were processed as described in Figure 3B. HMTase activity is inhibited by an unmodified $H3_{1–19}$ peptide (left), but not by H3K4me3- or H3K36me3-modified peptides.

(B) HMTase assay with H3Kc4me3-modified oligonucleosomes (36 nM), 86 nM PRC2, and H3K27me3 peptide in *trans*. Western blots were processed as described in Figure 3B. HMTase activity of PRC2 can be stimulated by the H3K27me3 peptide even on inhibiting substrate leading to increased levels of H3K27 di- and trimethylation.

modified peptides did not show this competitive behavior, we conclude that PRC2 is not inhibited by H3K4me3 in *trans* and that H3K4me3 and unmodified H3 peptides are probably bound to PRC2 in a different fashion. Analogously, we saw no inhibition when testing the effect of H3K4me3 in *trans* by using peptides as substrates (Figure S4B**)**. Taken together, our findings strongly argue that H3K4me3 only inhibits PRC2 if present on the same tail that contains the H3K27 target lysine (in *cis*).

Previous studies reported that addition of H3K27me3 peptides in *trans* enhances H3K27 methylation of oligonucleosomes by human PRC2 through binding to the EED WD40 domain (Margueron et al., 2009; Xu et al., 2010). We tested whether addition of H3K27me3 peptides in *trans* would stimulate H3K27 methylation by PRC2 on H3Kc4me3-modified nucleosomes. We observed that the inhibitory effect of H3Kc4me3-containing nucleosomes can, at least in part, be overcome through addition of high concentrations of H3K27me3 peptides (Figure 4B and Figure S4C). PRC2 is therefore able to simultaneously integrate inhibitory (H3K4me3) and activating (H3K27me3) chromatin signatures and adjust its enzymatic activity in response to the surrounding epigenetic environment.

PRC2 Inhibition of H3K4me3 Is Conserved in Mammalian PRC2

Our results with *Drosophila* PRC2 prompted us to investigate to what extent inhibition by H3K4me3 is an evolutionarily conserved mechanism. H3K27 methylation by human and mouse PRC2 on nucleosome substrates carrying H3Kc4me3 modifications was also strongly inhibited, comparable to the inhibition observed for *Drosophila* PRC2 (Figure 5A and Figure S5A).

The Su(z)12 Subunit Codetermines Whether PRC2 Is Inhibited by H3K4me3

In *Arabidopsis thaliana*, three different E(z) homologs combined with three Su(z)12 homologs have been described. The distinct PRC2 complexes in plants harboring the different E(z) or Su(z)12 subunits are implicated in the control of distinct developmental processes during *Arabidopsis* development (He, 2009). In this study we focused on PRC2 complexes containing the E(z) homolog CURLY LEAF (CLF). We expressed and reconstituted the *Arabidopsis* PRC2 complex comprising CLF, FERTILIZATION INDEPENDENT ENDOSPERM (FIE, a homolog of ESC), EMBRYONIC FLOWER 2 (EMF2, a homolog of Su(z)12), and MULTICOPY SUPPRESSOR OF IRA (MSI1, a homolog of Nurf55). We found that CLF indeed functions as a H3K27me3 HMTase (Figure 5B). Moreover, H3K27 methylation by the CLF-FIE-EMF2-MSI1 complex on nucleosome arrays containing H3Kc4me3 was inhibited (Figure 5B) in a manner comparable to human or *Drosophila* PRC2.

We next tested a related *Arabidopsis* PRC2 complex again composed of CLF, FIE, and MSI1 but containing the Su(z)12 homolog vernalization 2 (VRN2) instead of EMF2. The VRN2 protein is specifically implicated as a repressor of the FLC locus, thereby controlling flowering time in response to vernalization (reviewed in Henderson and Dean, 2004). The CLF-FIE-MSI1-VRN2 complex was active on unmodified nucleosomes but, strikingly, it was not inhibited on H3Kc4me3-modified nucleosomes (Figure 5C). Substitution of a single subunit (i.e., EMF2 by VRN2) thus renders the complex nonresponsive to the H3K4 methylation state. While PRC2 inhibition by H3K4me3 appears hardwired in mammals and flies, in which only a single-Su(z)12 ortholog is present, *Arabidopsis* inhibition can be enabled or disabled through exchange of the Su(z)12 homolog.

The Su(z)12 C Terminus Harboring the VEFS Domain Is the Minimal Su(z)12 Domain Required for Activation and Active Mark Inhibition

The importance of the Su(z)12 subunit in active mark H3K4me3 inhibition prompted us to map the Su(z)12 domains required for inhibition. Previous findings showed that E(z) or E(z)-ESC in the absence of Su(z)12 is enzymatically inactive (Nekrasov et al., 2005). Moreover, the *VEFS* domain (Birve et al., 2001) was found to be the major E(z) binding domain (Ketel et al., 2005). We reconstituted mouse PRC2 complexes containing EZH2, EED, and either SUZ12 C_2H_2 domain + VEFS (residues 439–741) or SUZ12 VEFS alone (residues 552–741). Both of these minimal complexes were active in HMTase assays on nucleosomes (Figure 5D) but with lower activity than that of the full PRC2 complex. We therefore focused on formation of

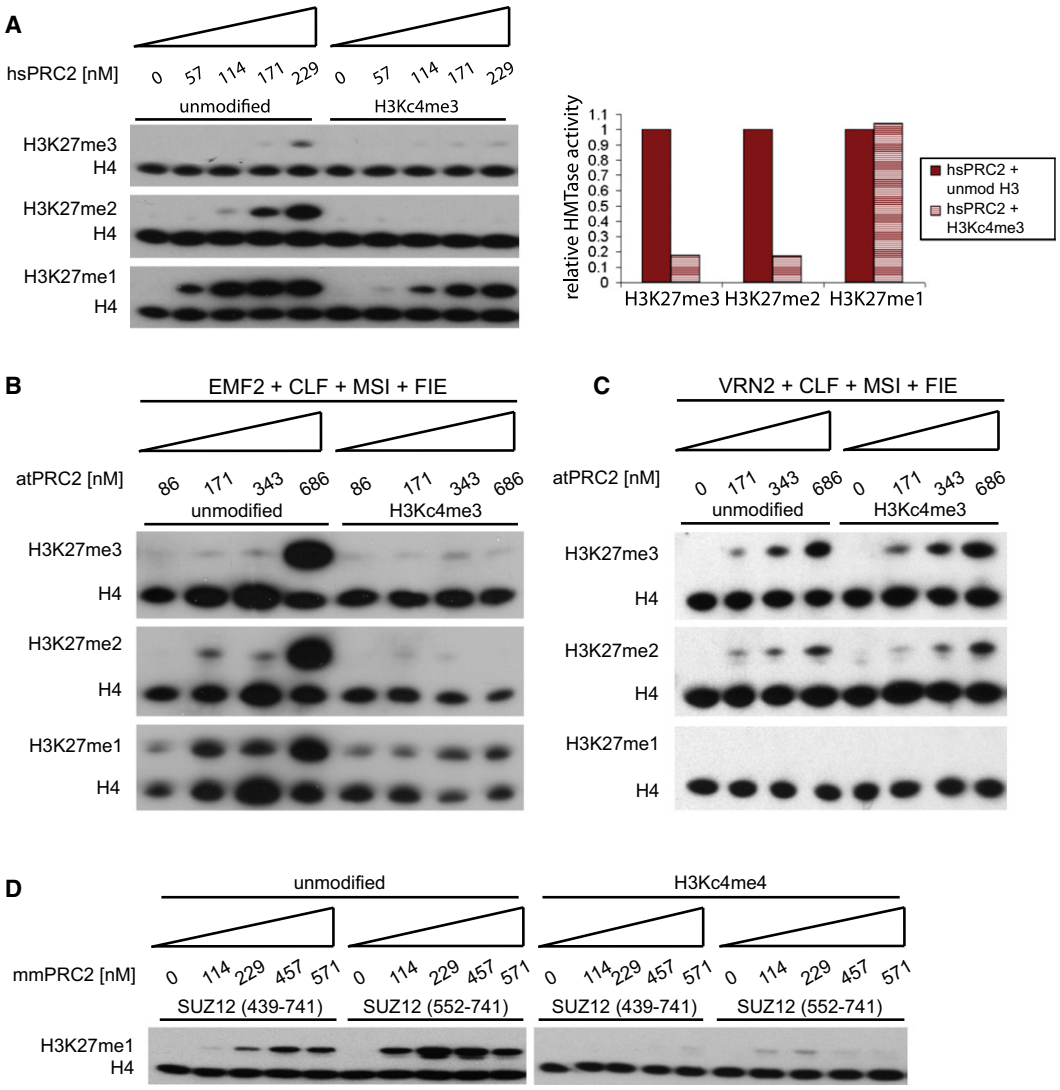

Figure 5. Sensitivity of PRC2 toward H3K4me3 Is Conserved in Mammals and Plants

(A) Left panel: Western blot-based HMTase assay with human PRC2 complex on unmodified and H3Kc4me3-modified mononucleosomes (571 nM). Western blots were processed as described in Figure 3B. Similar to the fly complex, human PRC2 is less active on H3Kc4me3 nucleosomes and H3K27 di- and trimethylation is severely hampered. Right panel: Quantification of HMTase activity of human PRC2 (286 nM) on unmodified and H3Kc4me3-modified nucleosomes by quantitative western blotting.

(B) HMTase assay with a plant PRC2 complex composed of EMF2, CLF, MSI1, and FIE on 4-mer oligonucleosomes (36 nM). Western blots were processed as described in Figure 3B. This complex is also sensitive to H3Kc4me3 and H3K27 di- and trimethylation on modified nucleosomes is severely reduced.

(C) HMTase assay with a plant PRC2 complex composed of VRN2, CLF, MSI1, and FIE on 4-mer oligonucleosomes (36 nM). Western blots were processed as described in Figure 3B. In contrast to the EMF2-containing complex, the VRN2 complex is insensitive toward H3Kc4me3 and has comparable activity on unmodified and modified nucleosomes.

(D) HMTase assay with mouse EZH2-EED-SUZ12 complexes containing truncated SUZ12 constructs (439–741 and 552–741) on 4-mer oligonucleosomes (36 nM). Western blots were processed as described in Figure 3B. Only the monomethylation signal is shown because the truncated SUZ12 complexes have poor HMTase activity. Both complexes remain inhibited by the H3Kc4me3 modification.

H3K27me1 as the strongest readout. When testing H3Kc4me3-containing nucleosomes, we found that both SUZ12 fragments rendered the complex sensitive to H3K4me3, resulting in the inhibition of H3K27 monomethylation (Figure 5D). The SUZ12 C terminus (including the VEFS domain) is thus the minimal SUZ12 fragment required for PRC2 binding, HMTase activity, and inhibition by H3K4me3.

Transcriptionally Active H3K36me2/3 Nucleosome Marks Also Inhibit PRC2

Finally, we asked whether other methylation marks associated with transcriptionally active chromatin but located outside the Nurf55-Su(z)12 binding site inhibit PRC2. We found that H3K27 methylation by PRC2 was also inhibited on H3Kc36me3 or H3Kc36me2 nucleosomes (Figure 6 and Figure S6). No

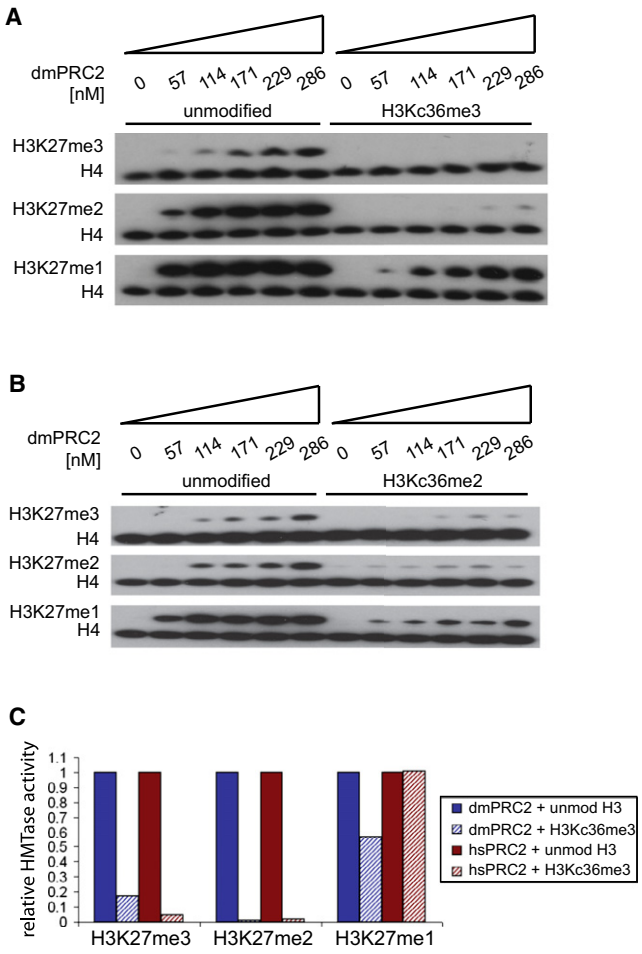

Figure 6. PRC2 Activity Is Also Inhibited by H3K36me2/3

(A) Western blot-based HMTase assay with *Drosophila* PRC2 complex on unmodified and H3Kc36me3-modified mononucleosomes (571 nM). Western blots were processed as described in Figure 3B. Similar to H3Kc4me3, H3Kc36me3 also inhibits the PRC2 complex.

(B) Same as in (A), western blot-based HMTase assay with *Drosophila* PRC2 complex, but with H3Kc36me2-modified nucleosomes.

(C) Quantitative western blot analysis estimating the HMTase activity of *Drosophila* (blue) and human (red) PRC2 complex (286 nM) on unmodified and H3Kc36me3-modified mononucleosomes.

significant inhibition was observed on control nucleosomes containing H3K36A or H3Kc36me0 lysine analog control (Figure S3E). As in the case of H3K4me3, inhibition by H3K36me2/3 could not be triggered by addition of the modified peptides, but required the modification to be present on the nucleosome containing the Lys27 substrate site (in *cis*) (Figure 4A). Moreover, we found that fly and human PRC2 were inhibited comparably. In the case of *Arabidopsis* PRC2, EMF2-containing complexes were inhibited by H3K36me3, whereas VRN2-containing complexes were not (Figure S6).

In conclusion, we find that three distinct histone methylation marks that are present in the coding region of actively transcribed genes—H3K4me3, H3K36me2, and H3K36me3—act as universal inhibitors of PRC2 complexes in both animals and plants.

DISCUSSION

Understanding how histone modification patterns are propagated during cell division is essential for understanding the molecular basis of epigenetic inheritance. Trimethylation of H3K27 by PRC2 has emerged as a key step in generating transcriptionally repressed chromatin in animals and plants. This study investigates how PRC2 recognizes the H3 tail and responds to H3-associated marks of active chromatin. Our crystallographic analyses reveal the molecular basis for $H3_{1-14}$ recognition by the Nurf55-Su(z)12 module of PRC2 and demonstrate that H3 tails carrying K4me3 are no longer recognized by Nurf55-Su(z)12. In the context of the whole PRC2 complex, H3K4me3 triggers allosteric inhibition of PRC2, a process that requires H3K4me3 to be present on the same histone molecule containing the substrate Lys27. We also observed PRC2 inhibition by H3K36me2/3. PRC2 inhibition by active chromatin marks (H3K4me3 and H3K36me2/3) is conserved in PRC2 complexes reconstituted from humans, mouse, flies, and plants.

The Role of Nurf55 in PRC2

Minimal PRC2 complexes lacking Nurf55 retain partial catalytic activity and are inhibited by H3K4me3 (Figure 5D). H3K4me3, once free of Nurf55, is thereby able to trigger PRC2 inhibition. We favor a model where Nurf55-Su(z)12 serves in sequestration and release of histone H3. We propose that the release of the H3 tail from Nurf55-Su(z)12 is required, but not sufficient, to induce H3K4me3 inhibition as it needs to trigger allosteric inhibition in conjunction with Su(z)12 and the E(z) SET domain (see below). Unmodified H3, H3K9me3, or H3R2me-modified tails, on the other hand, remain sequestered and are shielded from other chromatin factors. These sequestered marks are also not expected to interfere with PRC2 regulation. In line with this prediction, we observed that H3K9me3, which remained bound to Nurf55-Su(z)12, also did not interfere with PRC2 activity in vitro (Figure S5C). In vitro, binding of Nurf55 to the N terminus of H3 was not critical for the overall nucleosome binding affinity of PRC2 under our assay conditions (Figures S4A and S5B). However, small differences in PRC2 affinity amplified by large chromatin arrays could skew PRC2 recruitment toward sites of unmodified H3K4. Additionally, the Nurf55 interaction might play a more subtle role in positioning the complex correctly on nucleosomes.

Su(z)12 Mediates Inhibition by Active Marks in Conjunction with the E(z) SET Domain

Our in vitro findings suggest that active chromatin mark inhibition by PRC2 is largely governed through allosteric inhibition of the PRC2 HMTase activity thereby limiting processivity of the enzyme. We defined a minimal trimeric PRC2 subcomplex that retains both activity and H3K4me3/H3K36me2/3 inhibition. This minimal complex consists of ESC, an E(z) fragment that comprises the ESC binding region at the N terminus, the Su(z)12 binding domain in the middle (Hansen et al., 2008), and the C-terminal catalytic domain, and the Su(z)12 C terminus harboring the VEFS domain (Figure 5D). The importance of Su(z)12 is underlined by our findings on the *Arabidopsis* PRC2 complexes that revealed that active mark inhibition is determined by the choice of Su(z)12 subunit (i.e., inhibition with

EMF2, but not with VRN2) (Figures 5B and 5C). As the extent of methylation inhibition and the domains required for inhibition were similar for H3K4me3 and H3K36me2/3 (Figures 3 and 6), we hypothesize that both peptides function through a related mechanism allosterically affecting E(z) SET domain processivity with the help of Su(z)12. Further structural studies are required to reveal how these active marks are recognized and how this recognition is linked to inhibition of the E(z) SET domain.

PRC2 Mediates Crosstalk between Active and Repressive Histone Methylation Marks

H3K27me3 recognition by PRC2 has been reported to recruit and stimulate PRC2 (Hansen et al., 2008; Margueron et al., 2009), a mechanism implicated in creating and maintaining the extended H3K27me3 domains at target genes in vivo (Bernstein et al., 2006; Pan et al., 2007; Papp and Müller, 2006; Schwartz et al., 2006). Such positive feedback, however, necessitates a boundary element curtailing the expansion of H3K27me3. Our results suggest that actively transcribed genes (i.e., marked with H3K4me3 and H3K36me2/3) that flank domains of H3K27me3 chromatin may represent such boundary elements. In conjunction with H3K27me3-mediated stimulation, this provides a model how PRC2 could template domains of H3K27me3 chromatin during replication without expanding H3K27me3 domains into the chromatin of active genes. The inhibitory circuitry present in PRC2, however, does not function as a binary ON/OFF switch. PRC2 is able to integrate opposing H3K4me3 and H3K27me3 modifications into an intermediary H3K27 methylation activity (Figure 4B).

PRC2-Mediated Interdependence of H3K4me3/H3K36me3 versus H3K27me3 In Vivo

The crosstalk between H3K4me3 and H3K36me2/3 versus H3K27me3 has been extensively studied in vivo. Specifically, HOX genes in developing *Drosophila* larvae, or in mouse embryos, show mutually exclusive H3K27me3 and H3K4me3 domains that correlate with transcriptional OFF and ON states, respectively (Papp and Müller, 2006). In *Drosophila*, maintenance of HOX genes in the ON state critically depends on the trxG regulators Trx and Ash1, which methylate H3K4 and H3K36, respectively (Smith et al., 2004; Tanaka et al., 2007). At the *Ultrabithorax* (*Ubx*) gene, lack of Ash1 results in PRC2-dependent H3K27me3 deposition in the coding region of the normally active gene and the concomitant loss of *Ubx* transcription (Papp and Müller, 2006). Similarly, in the *Arabidopsis Flowering Locus C* (*FLC*), CLF-dependent deposition of H3K27me3 reduces H3K4me3 levels (Jiang et al., 2008), while deletion of the H3K4me3 demethylase *FLD* increases H3K4me3 levels and concomitantly diminishes H3K27me3 levels (Yu and Michaels, 2010). Our results provide a simple mechanistic explanation for these observations in plants and flies. We propose that H3K4 and H3K36 modifications in the coding region of active PcG target genes function as barriers that limit H3K27me3 deposition by PRC2.

Depositing Epigenetic Signatures-Knowing How to Stop?

We note that a number of HMTase complexes contain histone mark recognition domains that bind the very same mark that is deposited by their catalytic domain (Collins et al., 2008; Zhang et al., 2008; Chang et al., 2010). While this positive feedback loop guarantees the processivity of histone mark deposition, it also requires a control mechanism that avoids excessive spreading of marks. The direct inhibition of HMTases by histone marks, as seen for PRC2, may offer a paradigm of how excessive processivity can be counteracted in other HMTases.

Active Mark Inhibition Can Be Deactivated

Arabidopsis VRN2 is implicated in the control of the *FLC* locus after cold shock (reviewed in He, 2009). *FLC* is a bivalent locus containing both repressive H3K27me3 and active H3K4me3 marks (Jiang et al., 2008). In a VRN2-dependent fashion, H3K27me3 levels increase at *FLC* during vernalization. We find that while EMF2-containing PRC2 complexes are sensitive to H3K4me3 and H3K36me3, their VRN2-containing counterparts are not. In response to environmental stimuli plant PRC2 H3K4me3/H3K36me3 inhibition can thus be switched OFF (or ON). This offers the possibility that inhibition in animal PRC2 could also be modulated either by posttranslational modification of SUZ12 or by association with accessory factors.

PRC2 Inhibition and Coexistence of Active and Repressive Histone Methylation Marks

Quantitative mass spectrometry analyses of posttranslational modifications on the H3 N terminus in HeLa cells found no evidence for significant coexistence of H3K27me3 with H3K4me3 on the same H3 molecule (Young et al., 2009). Similarly, the fraction of H3 carrying both H3K27me3 and H3K36me3 was reported to be extremely low (~0.078%), while H3K27me3 and H3K36me2 coexist on ~1.315% of H3 molecules. However, H3K27me3/H3K4me3 and H3K27me3/H3K36me2/3 bivalent domains have been reported to exist in embryonic stem cells, and they have been implicated to exist on the same nucleosome (Bernstein et al., 2006). Given that PRC2 is inhibited by active methylation marks, how then could such bivalent domains be generated? We envisage two main possibilities. First, PRC2 inhibition in vivo could be alleviated by specific posttranslational modifications on PRC2 in embryonic stem cells (see in plants, VRN2). Second, H3K27me3 could be deposited prior to modification of H3K4 or H3K36. According to this view, one would have to postulate that the HMTases depositing H3K4me3 or H3K36me2/3 can work on nucleosomes containing H3K27me3. In support of this view, we found that H3K36 methylation by an NSD2 catalytic fragment is not inhibited by H3K27me3 marks on a peptide substrate (data not shown).

In summary, we found that mammalian and fly PRC2 complexes are not only activated by H3K27me3 as was recently reported (Margueron et al., 2009; Xu et al., 2010), but they are also inhibited by H3K4me3 and H3K36me2/3. PRC2, as a single biochemical entity, can thus integrate the information provided by histone modifications with antagonistic roles in gene regulation. While the biological network overseeing crosstalk between active and repressive chromatin marks in vivo probably extends beyond PRC2, including other chromatin modifiers such as histone demethylases (e.g., see Yokoyama et al., 2010), we identified a regulatory logic switch in PRC2 that intrinsically

separates active and repressive chromatin domains. Given the dynamic nature of the nucleosome template that makes up eukaryotic chromosomes, this circuitry probably equips PRC2 with the necessary precision to heritably propagate a repressed chromatin state.

EXPERIMENTAL PROCEDURES

Protein Purification and Crystallization

PRC2 proteins were recombinantly expressed and purified as described in Scrima et al. (2008). All crystals were grown at 20–25°C by the hanging drop vapor diffusion method. For Nurf55-Su(z)12 crystallization, a coexpressed $Nurf55_{1–418}$ and $Su(z)12_{73–143}$ complex at 16 mg/ml was incubated for 10 min with 0.01% subtilisin prior to setup. Subsequently, 1 μl drops of protein solution were mixed with 1 μl of reservoir solution containing 100 mM potassium acetate and 2.1 M ammonium sulfate. For Nurf55-$H3_{1–19}$ crystallization, Nurf55 protein was incubated with a ~5-fold molar excess of the $H3_{1–19}$ peptide for 30 min prior to crystallization. One microliter drops of a 22 mg/ml protein solution were mixed with 1 μl of reservoir solution containing 100 mM sodium citrate (pH 5.4), 200 mM ammonium acetate, and 23% PEG 3350. A detailed description of the experimental procedures is available in the Supplemental Experimental Procedures.

Binding Experiments

ITC and FP measurements were carried out as described in Grimm et al. (2007) and Jacobs et al. (2004), respectively. A detailed description of the experimental procedures is available in the Supplemental Experimental Procedures.

Nucleosome Assembly and Histone Methyltransferase Assay

Recombinant histones were expressed and purified (Luger et al., 1999) and site-specific methylation reactions were carried out as described in Simon (2010) and Simon et al. (2007). Histone octamers were reconstituted and purified as described in Luger et al. (1999) and assembled into nucleosomes by using the 601 sequence (Thåström et al., 1999) during stepwise salt dilution by dialysis. For the HMTase reaction mononucleosomes or 4-mer oligonucleosomes were incubated with the indicated amounts of PRC2 for 2 hr at 25°C in the presence of S-adenosyl methionine and reaction products were analyzed by western blotting. A detailed description of the experimental procedures is available in the Supplemental Experimental Procedures.

ACCESSION NUMBERS

The coordinates for the Nurf55-H3 and the Nurf55-Su(z)12 complex have been deposited in the PDB under ID codes 2YBA and 2YB8, respectively.

SUPPLEMENTAL INFORMATION

Supplemental Information includes six figures and Supplemental Experimental Procedures and can be found with this article online at doi:10.1016/j.molcel.2011.03.025.

ACKNOWLEDGMENTS

We thank Dirk Schübeler, Antoine Peters, and Susan Gasser for helpful discussions. We thank Norman Kairies and Andrea Scrima for crystallographic support, Maja Koehn and Victoria McParland for advice on peptide synthesis and purification, and Vladimir Rybin for help with ITC measurements. We are also grateful to Ernest Laue for providing us with the plasmid for the GST-H4 construct. Funding in the laboratory of N.H.T. is provided by Association for International Cancer Research grant 10-0292 and the Novartis Research Foundation. F.W.S. gratefully acknowledges funding from the Schering Foundation and the Studienstiftung des deutschen Volkes. A.B.P., N.L.-H., and J.M. were supported by European Molecular Biology Laboratory.

Received: June 14, 2010
Revised: December 8, 2010
Accepted: March 18, 2011
Published: May 5, 2011

REFERENCES

Beisel, C., Imhof, A., Greene, J., Kremmer, E., and Sauer, F. (2002). Histone methylation by the Drosophila epigenetic transcriptional regulator Ash1. Nature *419*, 857–862.

Bell, O., Conrad, T., Kind, J., Wirbelauer, C., Akhtar, A., and Schübeler, D. (2008). Transcription-coupled methylation of histone H3 at lysine 36 regulates dosage compensation by enhancing recruitment of the MSL complex in Drosophila melanogaster. Mol. Cell. Biol. *28*, 3401–3409.

Bernstein, B.E., Mikkelsen, T.S., Xie, X., Kamal, M., Huebert, D.J., Cuff, J., Fry, B., Meissner, A., Wernig, M., Plath, K., et al. (2006). A bivalent chromatin structure marks key developmental genes in embryonic stem cells. Cell *125*, 315–326.

Birve, A., Sengupta, A.K., Beuchle, D., Larsson, J., Kennison, J.A., Rasmuson-Lestander, A., and Müller, J. (2001). Su(z)12, a novel Drosophila Polycomb group gene that is conserved in vertebrates and plants. Development *128*, 3371–3379.

Cao, R., Wang, H., He, J., Erdjument-Bromage, H., Tempst, P., and Zhang, Y. (2008). Role of hPHF1 in H3K27 methylation and Hox gene silencing. Mol. Cell. Biol. *28*, 1862–1872.

Cao, R., Wang, L., Wang, H., Xia, L., Erdjument-Bromage, H., Tempst, P., Jones, R.S., and Zhang, Y. (2002). Role of histone H3 lysine 27 methylation in Polycomb-group silencing. Science *298*, 1039–1043.

Chang, P.Y., Hom, R.A., Musselman, C.A., Zhu, L., Kuo, A., Gozani, O., Kutateladze, T.G., and Cleary, M.L. (2010). Binding of the MLL PHD3 finger to histone H3K4me3 is required for MLL-dependent gene transcription. J. Mol. Biol. *400*, 137–144.

Collins, R.E., Northrop, J.P., Horton, J.R., Lee, D.Y., Zhang, X., Stallcup, M.R., and Cheng, X. (2008). The ankyrin repeats of G9a and GLP histone methyltransferases are mono- and dimethyllysine binding modules. Nat. Struct. Mol. Biol. *15*, 245–250.

Czermin, B., Melfi, R., McCabe, D., Seitz, V., Imhof, A., and Pirrotta, V. (2002). Drosophila enhancer of Zeste/ESC complexes have a histone H3 methyltransferase activity that marks chromosomal Polycomb sites. Cell *111*, 185–196.

Dong, A., Xu, X., Edwards, A.M., Chang, C., Chruszcz, M., Cuff, M., Cymborowski, M., Di Leo, R., Egorova, O., Evdokimova, E., et al; Midwest Center for Structural Genomics; Structural Genomics Consortium. (2007). In situ proteolysis for protein crystallization and structure determination. Nat. Methods *4*, 1019–1021.

Gaudet, R., Bohm, A., and Sigler, P.B. (1996). Crystal structure at 2.4 angstroms resolution of the complex of transducin betagamma and its regulator, phosducin. Cell *87*, 577–588.

Grimm, C., de Ayala Alonso, A.G., Rybin, V., Steuerwald, U., Ly-Hartig, N., Fischle, W., Müller, J., and Müller, C.W. (2007). Structural and functional analyses of methyl-lysine binding by the malignant brain tumour repeat protein Sex comb on midleg. EMBO Rep. *8*, 1031–1037.

Hansen, K.H., Bracken, A.P., Pasini, D., Dietrich, N., Gehani, S.S., Monrad, A., Rappsilber, J., Lerdrup, M., and Helin, K. (2008). A model for transmission of the H3K27me3 epigenetic mark. Nat. Cell Biol. *10*, 1291–1300.

He, Y. (2009). Control of the transition to flowering by chromatin modifications. Mol Plant *2*, 554–564.

Henderson, I.R., and Dean, C. (2004). Control of Arabidopsis flowering: the chill before the bloom. Development *131*, 3829–3838.

Jacobs, S.A., Fischle, W., and Khorasanizadeh, S. (2004). Assays for the determination of structure and dynamics of the interaction of the chromodomain with histone peptides. Methods Enzymol. *376*, 131–148.

Jiang, D., Wang, Y., Wang, Y., and He, Y. (2008). Repression of FLOWERING LOCUS C and FLOWERING LOCUS T by the Arabidopsis Polycomb repressive complex 2 components. PLoS ONE *3*, e3404.

Ketel, C.S., Andersen, E.F., Vargas, M.L., Suh, J., Strome, S., and Simon, J.A. (2005). Subunit contributions to histone methyltransferase activities of fly and worm polycomb group complexes. Mol. Cell. Biol. *25*, 6857–6868.

Kuzmichev, A., Jenuwein, T., Tempst, P., and Reinberg, D. (2004). Different EZH2-containing complexes target methylation of histone H1 or nucleosomal histone H3. Mol. Cell *14*, 183–193.

Luger, K., Mäder, A.W., Richmond, R.K., Sargent, D.F., and Richmond, T.J. (1997). Crystal structure of the nucleosome core particle at 2.8 A resolution. Nature *389*, 251–260.

Luger, K., Rechsteiner, T.J., and Richmond, T.J. (1999). Expression and purification of recombinant histones and nucleosome reconstitution. Methods Mol. Biol. *119*, 1–16.

Margueron, R., Justin, N., Ohno, K., Sharpe, M.L., Son, J., Drury, W.J., 3rd, Voigt, P., Martin, S.R., Taylor, W.R., De Marco, V., et al. (2009). Role of the polycomb protein EED in the propagation of repressive histone marks. Nature *461*, 762–767.

Milne, T.A., Briggs, S.D., Brock, H.W., Martin, M.E., Gibbs, D., Allis, C.D., and Hess, J.L. (2002). MLL targets SET domain methyltransferase activity to Hox gene promoters. Mol. Cell *10*, 1107–1117.

Müller, J., Hart, C.M., Francis, N.J., Vargas, M.L., Sengupta, A., Wild, B., Miller, E.L., O'Connor, M.B., Kingston, R.E., and Simon, J.A. (2002). Histone methyltransferase activity of a Drosophila Polycomb group repressor complex. Cell *111*, 197–208.

Murzina, N.V., Pei, X.Y., Zhang, W., Sparkes, M., Vicente-Garcia, J., Pratap, J.V., McLaughlin, S.H., Ben-Shahar, T.R., Verreault, A., Luisi, B.F., and Laue, E.D. (2008). Structural basis for the recognition of histone H4 by the histone-chaperone RbAp46. Structure *16*, 1077–1085.

Nakamura, T., Mori, T., Tada, S., Krajewski, W., Rozovskaia, T., Wassell, R., Dubois, G., Mazo, A., Croce, C.M., and Canaani, E. (2002). ALL-1 is a histone methyltransferase that assembles a supercomplex of proteins involved in transcriptional regulation. Mol. Cell *10*, 1119–1128.

Nekrasov, M., Klymenko, T., Fraterman, S., Papp, B., Oktaba, K., Köcher, T., Cohen, A., Stunnenberg, H.G., Wilm, M., and Müller, J. (2007). Pcl-PRC2 is needed to generate high levels of H3-K27 trimethylation at Polycomb target genes. EMBO J. *26*, 4078–4088.

Nekrasov, M., Wild, B., and Müller, J. (2005). Nucleosome binding and histone methyltransferase activity of Drosophila PRC2. EMBO Rep. *6*, 348–353.

Pan, G., Tian, S., Nie, J., Yang, C., Ruotti, V., Wei, H., Jonsdottir, G.A., Stewart, R., and Thomson, J.A. (2007). Whole-genome analysis of histone H3 lysine 4 and lysine 27 methylation in human embryonic stem cells. Cell Stem Cell *1*, 299–312.

Papp, B., and Müller, J. (2006). Histone trimethylation and the maintenance of transcriptional ON and OFF states by trxG and PcG proteins. Genes Dev. *20*, 2041–2054.

Pasini, D., Bracken, A.P., Jensen, M.R., Lazzerini Denchi, E., and Helin, K. (2004). Suz12 is essential for mouse development and for EZH2 histone methyltransferase activity. EMBO J. *23*, 4061–4071.

Pietersen, A.M., and van Lohuizen, M. (2008). Stem cell regulation by polycomb repressors: postponing commitment. Curr. Opin. Cell Biol. *20*, 201–207.

Santos-Rosa, H., Schneider, R., Bannister, A.J., Sherriff, J., Bernstein, B.E., Emre, N.C., Schreiber, S.L., Mellor, J., and Kouzarides, T. (2002). Active genes are tri-methylated at K4 of histone H3. Nature *419*, 407–411.

Sarma, K., Margueron, R., Ivanov, A., Pirrotta, V., and Reinberg, D. (2008). Ezh2 requires PHF1 to efficiently catalyze H3 lysine 27 trimethylation in vivo. Mol. Cell. Biol. *28*, 2718–2731.

Schuettengruber, B., Chourrout, D., Vervoort, M., Leblanc, B., and Cavalli, G. (2007). Genome regulation by polycomb and trithorax proteins. Cell *128*, 735–745.

Schwartz, Y.B., Kahn, T.G., Nix, D.A., Li, X.Y., Bourgon, R., Biggin, M., and Pirrotta, V. (2006). Genome-wide analysis of Polycomb targets in Drosophila melanogaster. Nat. Genet. *38*, 700–705.

Schwartz, Y.B., and Pirrotta, V. (2007). Polycomb silencing mechanisms and the management of genomic programmes. Nat. Rev. Genet. *8*, 9–22.

Scrima, A., Konícková, R., Czyzewski, B.K., Kawasaki, Y., Jeffrey, P.D., Groisman, R., Nakatani, Y., Iwai, S., Pavletich, N.P., and Thomä, N.H. (2008). Structural basis of UV DNA-damage recognition by the DDB1-DDB2 complex. Cell *135*, 1213–1223.

Shogren-Knaak, M.A., Fry, C.J., and Peterson, C.L. (2003). A native peptide ligation strategy for deciphering nucleosomal histone modifications. J. Biol. Chem. *278*, 15744–15748.

Simon, M.D. (2010). Installation of site-specific methylation into histones using methyl lysine analogs. In Current Protocols in Molecular Biology, Ausubel, F.M., et al., eds. (Hoboken, NJ: John Wiley & Sons), Unit 21.18.1–21.18.10.

Simon, M.D., Chu, F., Racki, L.R., de la Cruz, C.C., Burlingame, A.L., Panning, B., Narlikar, G.J., and Shokat, K.M. (2007). The site-specific installation of methyl-lysine analogs into recombinant histones. Cell *128*, 1003–1012.

Smith, S.T., Petruk, S., Sedkov, Y., Cho, E., Tillib, S., Canaani, E., and Mazo, A. (2004). Modulation of heat shock gene expression by the TAC1 chromatin-modifying complex. Nat. Cell Biol. *6*, 162–167.

Song, J.J., Garlick, J.D., and Kingston, R.E. (2008). Structural basis of histone H4 recognition by p55. Genes Dev. *22*, 1313–1318.

Srinivasan, S., Dorighi, K.M., and Tamkun, J.W. (2008). Drosophila Kismet regulates histone H3 lysine 27 methylation and early elongation by RNA polymerase II. PLoS Genet. *4*, e1000217.

Tanaka, Y., Katagiri, Z., Kawahashi, K., Kioussis, D., and Kitajima, S. (2007). Trithorax-group protein ASH1 methylates histone H3 lysine 36. Gene *397*, 161–168.

Thåström, A., Lowary, P.T., Widlund, H.R., Cao, H., Kubista, M., and Widom, J. (1999). Sequence motifs and free energies of selected natural and non-natural nucleosome positioning DNA sequences. J. Mol. Biol. *288*, 213–229.

Verreault, A., Kaufman, P.D., Kobayashi, R., and Stillman, B. (1998). Nucleosomal DNA regulates the core-histone-binding subunit of the human Hat1 acetyltransferase. Curr. Biol. *8*, 96–108.

Wu, J.I., Lessard, J., and Crabtree, G.R. (2009). Understanding the words of chromatin regulation. Cell *136*, 200–206.

Wysocka, J., Swigut, T., Xiao, H., Milne, T.A., Kwon, S.Y., Landry, J., Kauer, M., Tackett, A.J., Chait, B.T., Badenhorst, P., et al. (2006). A PHD finger of NURF couples histone H3 lysine 4 trimethylation with chromatin remodelling. Nature *442*, 86–90.

Xu, C., Bian, C., Yang, W., Galka, M., Ouyang, H., Chen, C., Qiu, W., Liu, H., Jones, A.E., Mackenzie, F., et al. (2010). Binding of different histone marks differentially regulates the activity and specificity of polycomb repressive complex 2 (PRC2). Proc. Natl. Acad. Sci. U. S. A. *107*, 19266–19271.

Yokoyama, A., Okuno, Y., Chikanishi, T., Hashiba, W., Sekine, H., Fujiki, R., and Kato, S. (2010). KIAA1718 is a histone demethylase that erases repressive histone methyl marks. Genes Cells *15*, 867–873.

Young, N.L., DiMaggio, P.A., Plazas-Mayorca, M.D., Baliban, R.C., Floudas, C.A., and Garcia, B.A. (2009). High throughput characterization of combinatorial histone codes. Mol. Cell. Proteomics *8*, 2266–2284.

Yu, X., and Michaels, S.D. (2010). The Arabidopsis Paf1c complex component CDC73 participates in the modification of FLOWERING LOCUS C chromatin. Plant Physiol. *153*, 1074–1084.

Zhang, K., Mosch, K., Fischle, W., and Grewal, S.I. (2008). Roles of the Clr4 methyltransferase complex in nucleation, spreading and maintenance of heterochromatin. Nat. Struct. Mol. Biol. *15*, 381–388.